**NASA TECHNICAL MEMORANDUM**

**NASA TM X-74017**

NASA TM X-74017

# INCLUSION OF EXPLICIT THERMAL REQUIREMENTS IN OPTIMUM STRUCTURAL DESIGN

(NASA-TM-X-74017) INCLUSION OF EXPLICIT THERMAL REQUIREMENTS IN OPTIMUM STRUCTURAL DESIGN (NASA) 41 p HC A03/MF A01 CSCL 13M

N77-21469

Unclas
G3/39 24430

Howard M. Adelman

and

Patricia L. Sawyer

March 1977



National Aeronautics and Space Administration

Langley Research Center
Hampton, Virginia 23665

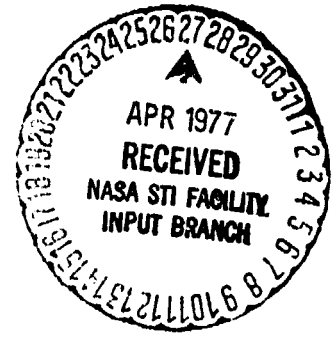

| 1. Report No. | 2. Government Accession No. | 3. Recipient's Catalog No. |
|---|---|---|
| NASA TM X-74017 | | |

| 4. Title and Subtitle | 5. Report Date |
|---|---|
| INCLUSION OF EXPLICIT THERMAL REQUIREMENTS IN OPTIMUM STRUCTURAL DESIGN | March 1977 |
| | 6. Performing Organization Code |

| 7. Author(s) | 8. Performing Organization Report No. |
|---|---|
| Howard M. Adelman and Patricia L. Sawyer | |
| | 10. Work Unit No. 743-01-11-03 |
| 9. Performing Organization Name and Address | 11. Contract or Grant No. |
| NASA Langley Research Center<br>Hampton, Virginia 23665 | |
| | 13. Type of Report and Period Covered |
| 12. Sponsoring Agency Name and Address | Technical Memorandum |
| National Aeronautics and Space Administration<br>Washington, DC 20546 | 14. Sponsoring Agency Code |

15. Supplementary Notes

16. Abstract

A finite-element based procedure is described for obtaining minimum mass designs of structures subjected to combined thermal and mechanical loading and both strength and thermal constraints. The procedure is based on a mathematical programming method using the Sequence of Unconstrained Minimizations Technique (SUMT) in which design requirements are incorporated by an exterior penalty function. Temperatures are treated as behavior variables rather than fixed load-type quantities and are recalculated during the resizing process using a finite element thermal analysis. The procedure is limited to steady-state temperatures which are controlled by structural sizing only. The optimization procedure is demonstrated by the design of a structural wing box with both mechanical loading and external heating, subject to design constraints on stress, minimum gage, and temperature. The final design for these conditions is compared with a corresponding design in which temperature constraints are omitted. Temperature constraints have a significant effect on both the distribution of structural material and the total mass in the final design.

Some additional developments beyond the scope of the present work but needed for design of practical aerospace structures under realistic load situations are identified. Among these developments are design-oriented transient thermal analysis capability, treatment of time-dependent constraints and incorporation of effective temperature control devices and thermal-stress relieving mechanisms.

| 17. Key Words (Suggested by Author(s)) | 18. Distribution Statement |
|---|---|
| Optimum Structural Design<br>Thermal Stress<br>Mathematical Programming<br>Thermal Analysis<br>Thermal Requirements | UNCLASSIFIED - UNLIMITED<br><br>Subject Category 39 |

| 19. Security Classif. (of this report) | 20. Security Classif. (of this page) | 21. No. of Pages | 22. Price* |
|---|---|---|---|
| UNCLASSIFIED | UNCLASSIFIED | 39 | $4.00 |

* For sale by the National Technical Information Service, Springfield, Virginia 22161

# INCLUSION OF EXPLICIT THERMAL REQUIREMENTS IN OPTIMUM STRUCTURAL DESIGN

By Howard M. Adelman and Patricia L. Sawyer
Langley Research Center

## SUMMARY

A finite-element based procedure is described for obtaining minimum mass designs of structures subjected to combined thermal and mechanical loading and both strength and thermal constraints. The procedure is based on a mathematical programming method using the Sequence of Unconstrained Minimizations Technique (SUMT) in which design requirements are incorporated by an exterior penalty function. Temperatures are treated as behavior variables rather than fixed load-type quantities and are recalculated during the resizing process using a finite element thermal analysis. The procedure is limited to steady-state temperatures which are controlled by structural sizing only. The optimization procedure is demonstrated by the design of a structural wing box with both mechanical loading and external heating, subject to design constraints on stress, minimum gage, and temperature. The final design for these conditions is compared with a corresponding design in which temperature constraints are omitted. Temperature constraints have a significant effect on both the distribution of structural material and the total mass in the final design.

Some additional developments beyond the scope of the present work but needed for design of practical aerospace structures under realistic load situations are identified. Among these developments are design-oriented transient thermal analysis capability, treatment of time-dependent constraints and incorporation of effective temperature control devices and thermal-stress relieving mechanisms.

## INTRODUCTION

The necessity for light-weight aerospace vehicles to withstand both mechanical loading and severe thermal environments during atmospheric entry

and hypersonic cruise has led to the problem of designing minimum-mass structures that must satisfy both mechanical and thermal design requirements. Mechanical requirements to insure structural integrity include limits on stress, buckling loads and flutter speed. Thermal requirements to avoid material property degradation and excessive temperatures in cargo and crew compartments consist of upper limits on structural temperatures.

Previous structural synthesis work has generally concentrated on designing structures under mechanical loads for mechanical requirements. Thermal loads were incorporated as specified structural temperatures supplied by an independent thermal analysis and equivalent loads were added to the applied mechanical loads (ref. 1-3). Temperatures entered into the synthesis problem indirectly through the strength requirements and explicit thermal requirements were not included. The temperatures of points on the structures were not recalculated as the structure was resized. Thus, good initial estimates of the structural member sizes were required to avoid significant differences between the temperature distributions in the initial and final designs.

Two logical improvements to existing thermal-structural design methods are incorporation of temperature constraints and recalculation of temperatures during resizing. Early recognition of the need for these features is reflected in reference 4 which describes the optimization of an ablating heat shield with upper limits on temperature, and reference 5 which indicates the importance of recalculating temperatures of structural elements during resizing. The purpose of the present work is to combine the aforementioned techniques for thermal optimization with state-of-the-art techniques for finite-element based structural optimization to produce a coupled thermal-mechanical optimization procedure.

It is recognized that a complete and practical structural synthesis method should include design-oriented transient thermal analysis capability and the associated treatment of time-dependent constraints. Design variables for thermal control (insulation thickness, parameters of heat pipes and convective cooling systems) as well as parameters of thermal-stress relief devices (expansion joints) should be included in the procedure. Although consideration of such capability is discussed in the present paper, incorporation of these features into an optimization procedure is beyond the scope of the present work.

In the present paper, a simplified thermal-mechanical optimization procedure is presented based on steady-state structural temperatures and design variables consisting of thicknesses of membrane elements and cross-sectional areas of bar elements. The procedure is based on a standard nonlinear mathematical programming formulation using the Sequence of Unconstrained Minimizations Techniques (SUMT) in which design requirements are incorporated with an exterior penalty function. Calculations of temperatures and stresses during resizing are performed by finite element analyses using one- and two-dimensional elements. Design requirements include limits on element stresses, temperatures and minimum gage. The procedure is demonstrated by the minimum-mass design of a wing box under combined mechanical loading and external heating. Designs are obtained with and without temperature constraints in order to indicate the effects of these requirements.

## SYMBOLS

| | |
|---|---|
| $A$ | area of a bar element |
| $A_{min}$ | bar minimum gage area |
| $[B]$ | row vector relating stress in a bar to displacement |
| $[C_x]$, $[C_y]$, $[C_{xy}]$ | row vectors relating membrane stresses to displacements |
| $E$ | Young's modulus |
| $G_x$, $G_y$, $G_{xy}$ | factors relating membrane thermal stresses to temperatures |
| $g$ | design constraint |
| $H$ | convective heat transfer coefficient |
| $h$ | membrane thickness |
| $h_{min}$ | membrane minimum gage thickness |
| $[K]$ | stiffness matrix |
| $[\bar{K}]$ | conductivity matrix |
| $k$ | thermal conductivity |
| $\{L\}$ | structural load vector |

| | |
|---|---|
| $\{\bar{L}\}$ | thermal load vector |
| m | mass of structure |
| $N_x$, $N_y$, $N_{xy}$ | forces per unit length (fig. 1) |
| nb | number of bar elements in finite element model |
| nc | number of design constraints |
| nm | number of membrane elements in finite element model |
| p | pressure |
| Q, q | heat flux |
| r | penalty function weighting factor |
| {T} | vector of structural temperatures |
| $\bar{T}$ | temperature of a bar or membrane element |
| {t} | vector of design variables |
| {U} | displacement vector for structure |
| {u} | displacement vector for bar or membrane element |
| u, v, w | displacement components in X-, Y-, and Z-directions, respectively |
| V | $[\sigma^2_x + \sigma^2_y - \sigma_x\sigma_y + 3\sigma^2_{xy}]^{1/2}$, Von Mises stress measure |
| X-, Y-, Z- | global coordinate directions (fig. 2) |
| x, y | Cartesian coordinate directions in plane of membrane element |
| $\alpha$ | coefficient of linear thermal expansion |
| $\phi$ | penalty function |
| $\sigma$ | bar stress |
| $\sigma_x$, $\sigma_y$, $\sigma_{xy}$ | membrane stress components |
| $\tau$ | time |

Subscripts:

| | |
|---|---|
| a | allowable |
| b | bar |
| i | index indicating discrete time or design variable (Appendix B) |
| j | index indicating constraint number |
| m | membrane |

## DESIGN METHOD

### Overall Approach

The objective of the design method is to determine a structural design having minimum mass and satisfying the requirements that the structural elements have stress levels within specified limits, temperatures below specified values, and structural sizes above minimum values. The approach is to formulate and solve a nonlinear mathematical programming problem based on the Sequence of Unconstrained Minimizations Technique in which constraints are represented by an exterior penalty function (ref. 6). Calculations of stresses and temperatures are performed using finite element analyses.

### Structural Analysis

Calculations of displacements and stresses are carried out using bar finite elements and triangular membrane elements having mid-side grid points (ref. 7). Pertinent equations used in the structural analysis and needed for gradient calculations are as follows:

Equilibrium equation:

$$[K]\{U\} = \{L\} \tag{1}$$

Bar constitutive equation:

$$\sigma_b = [B]\{u\}_b - E_b\alpha_b\overline{T}_b \tag{2}$$

Membrane constitutive equation:

$$\begin{Bmatrix} \sigma_x \\ \sigma_y \\ \sigma_{xy} \end{Bmatrix} = \begin{bmatrix} [C_x] \\ [C_y] \\ [C_{xy}] \end{bmatrix} \{u\}_m - \begin{bmatrix} G_x \\ G_y \\ G_{xy} \end{bmatrix} \bar{T}_m \tag{3}$$

The measure of stress in the membranes is the Von Mises stress V, given by

$$V = [\sigma^2_x + \sigma^2_y - \sigma_x\sigma_y + 3\sigma^2_{xy}]^{1/2} \tag{4}$$

## Thermal Analysis

Temperatures are calculated using the same finite element model used for the structural analysis. One-dimensional elements incorporate conduction along the length and also allow for convective heat transfer and constant heat loads applied to the element. The temperature is assumed to vary linearly along the element length. The two-dimensional elements incorporate conduction in the plane of the element and allow for heat loads normal to the plane of the element as well as normal to the sides of the element. The temperature is assumed to vary quadratically in the plane of the element and the temperature is uniform through the thickness.

The equation for calculating structural temperatures is:

$$[\bar{K}] \{T\} = \{\bar{L}\} \tag{5}$$

where $[\bar{K}]$ is the conductivity matrix for the structure, $\{T\}$ is the vector of grid point temperatures, and $\{\bar{L}\}$ is the thermal force vector for the structure including contributions from convective heating and prescribed heat flux. The conductivity matrices and thermal load vectors for membrane and bar elements are derived for a general set of thermal loads in Appendix A.

## Optimization Method

Problem definition and solution. - The optimization problem consists of determining a vector of design variables $\{t\}$ which minimizes the mass of the structure $m$, subject to a set of constraints $\{g\}$. The problem is solved by the Sequence of Unconstrained Minimizations Technique in which constraints are incorporated by an exterior penalty function. Thus, the problem is formally posed as follows:

$$\text{Minimize} \quad \phi = m + r \sum_{j=1}^{nc} \langle g_j \rangle^2 \tag{6}$$

for a sequence of increasing values of the weighting factor $r$. The unconstrained minimizations for each value of $r$ are carried out using a first-order Quasi-Newton method denoted Davidon's Second Method (ref. 8). Similar to the method of Davidon-Fletcher-Powell (ref.9), Davidon's Second Method requires only one evaluation of the function and gradient per iteration, and does not require a one-dimensional search to obtain the function minimum. The notation $\langle g_j \rangle$ is defined as follows:

$$\langle g_j \rangle = \begin{cases} 0 & \text{if} \quad g_j \geq 0 \\ g_j & \text{if} \quad g_j < 0 \end{cases} \tag{7}$$

Constraints. - Each design variable (area of bar or thickness of membrane) is subjected to stress, temperature, and minimum gage constraints. These are summarized as follows:

Bar stress: $$g = 1 - \sigma/\sigma_a \geq 0 \tag{8}$$

Bar minimum gage: $$g = 1 - A_{min}/A \geq 0 \tag{9}$$

Bar temperature: $g = 1 - \bar{T}/T_a \geq 0$ (10)

Membrane stress: $g = 1 - V/\sigma_a \geq 0$ (11)

Membrane minimum gage: $g = 1 - h_{min}/h \geq 0$ (12)

Membrane temperature: $g = 1 - \bar{T}/T_a \geq 0$ (13)

These functions are defined so that positive values correspond to satisfied constraints and negative values correspond to violated constraints. The total number of constraints is three times the number of structural elements. Expressions for components of the gradient of the constraints required during the optimization are derived in Appendix B.

## APPLICATION OF THE PROCEDURE TO MINIMUM MASS DESIGN OF WING BOX

### Model Description

The optimization procedure is demonstrated for a structure which requires finite element analysis but is simple enough to avoid a host of modeling details. The structure, loading, and design requirements have been selected to demonstrate salient features of the techniques and ideas developed in this paper. The overall structural configuration shown in figure 1 consists of upper and lower covers, 4 ribs and 3 spars. The loading includes in-plane forces per unit length $N_x$, $N_y$, and $N_{xy}$, as well as pressure over the upper and lower surfaces. In addition, a uniform heat flux is applied over the lower surface of the structure. Boundary conditions include prescribed temperatures on edges 1 through 4 and prescribed zero displacements on edges 3 and 4 (fig. 1). The thermal design requirements consist of an upper limit of 1090 K (1500°F) on the temperature of all structural elements. The allowable stress for all structural elements is 0.875 GPa (127 ksi). Minimum gage limitations are bar areas of 0.0064 $cm^2$ (0.01 $in^2$) and membrane thicknesses of 0.254 mm (0.01 in.). A summary of loads, boundary conditions, and material properties is given in table 1.

The finite element model for the structure is shown in figure 2. The ribs

and spars are modeled by trusses and the covers are modeled by membranes. Modeling details are shown in figure 3. The model consists of 68 bars, 8 membranes and 30 gridpoints resulting in an optimization problem with 76 design variables. Coordinates of the gridpoints are listed in table 2 and the forces resolved into gridpoint forces are given in table 3. The boundary conditions expressed in terms of the gridpoint temperatures and displacements are given in table 4.

## Determination of Optimum Design

Design with temperature constraints included. - The starting point for the optimization was a structure in which all structural elements were sized at minimum gage. This initial design had a mass of 39 kg (86 lbm) and had a large number of constraint violations. The optimum design was obtained after 12 unconstrained minimizations and had a mass of 486 kg (1070 lbm). The cross-sectional areas of the bars and thicknesses of the membranes in the optimum design are listed in table 5. The thicknesses of the membranes in the upper and lower skins are shown in figure 4. The thickest element of the skin (element 5) is in the lower surface adjacent to the built-in edge where the largest stresses occur, and this element is stress-critical. The next thickest element (element 7) is located at the interior of the lower surface where the highest temperatures occur, and this element is temperature-critical. A summary of the critical constraints is given in table 6(a). Of the 8 membrane elements used to represent the upper and lower skins, 3 are stress-critical, 3 are temperature-critical (all on the lower skin), and element 3 on the upper surface is sized at minimum gage. Element 2 has no active constraints.

Design with temperature constraints omitted. - In order to assess the effect of including temperature constraints, the wing box calculations were repeated with temperature constraints omitted. The starting design was a minimum-gage structure. The final design was obtained after 11 unconstrained minimizations and had a mass of 280 kg (617 lbm). This design is tabulated in table 7, and a list of the critical constraints is given in table 6(b). The distribution of skin thicknesses and identification of active constraints are shown in figure 5. The largest proportion of structural material is represented by element 5 in the lower skin. The most notable difference in the skin

designs with and without temperature constraints is the size of element 7 which was temperature-critical when the upper limit of 1090 K (1500°F) was enforced. In the present design, the temperature of element 7 is 1133 K (1580°F) and the element is significantly thinner. Omitting the constraint permitted the higher temperatures and reduced the need for element 7 to conduct heat to cooler parts of the structure. The differences between the masses of the designs with and without temperature constraints is largely due to the difference in mass of element 7. Membranes 6 and 8 which were also temperature-critical in the previous design, had temperatures in the current design of 1109 K (1536°F) and 1114 K (1545°F), respectively.

## CONSIDERATIONS FOR ADVANCED APPLICATIONS

Advanced applications of the design procedure of this paper require development of the following features and capabilities:

(1) design-oriented transient thermal analysis
(2) treatment of time-dependent constraints
(3) incorporation of effective temperature control devices
(4) incorporation of thermal-stress relieving mechanisms.

Each of these items is discussed in the succeeding paragraphs.

### Design-Oriented Transient Thermal Analysis

A most pressing need before optimization procedures can be applied to practical aerospace structures under realistic load situations is the incorporation of transient thermal analysis. While there are a variety of algorithms for tracing out time histories of temperatures (for example, ref. 10), such algorithms are typically iterative. Consequently, an iteration loop for thermal analysis must be embedded in the optimization iteration loop leading to potentially long and expensive computer runs. Design-oriented transient thermal analysis, perhaps based on Taylor series approximations in a manner similar to the analysis technique of references 1 and 11, has potential for efficient thermal optimization procedures. Additionally, the idea of updating temperatures only after selected design iterations (suggested in ref. 4) would reduce the total number of calculations. This technique should be especially

useful in the later stages of design where relatively small changes in the design variables occur and consequently, only small changes in the temperatures are expected.

## Time-Dependent Constraints

Because temperatures and stresses can be time-dependent, behavior constraints can be similarly time-dependent. Techniques are, therefore, needed for constraints such as

$$g(\tau) = 1 - \bar{T}(\tau)/T_a \tag{14}$$

where $\tau$ denotes time and $T_a$ is the allowable temperature. One method of dealing with this type of constraint is to replace it by the integrated average as in reference 4. Thus, the actual constraint on time-dependent temperature is replaced by

$$g = 1 - T^*/T_a \tag{15}$$

where

$$T^* = \frac{1}{T_f}\int_0^{T_f} \bar{T}(\tau)d\tau \tag{16}$$

and $T_f$ is the length of time over which the temperature is being monitored. As pointed out in reference 4, one drawback to this approach is that it tends to smooth the penalty function and thereby causes temperatures to be somewhat insensitive to changes in the design variables. An alternative approach is to satisfy the constraints at a finite number of discrete times (NT). Thus, the continuous time-varying constraint of equation (14) is replaced by the following constraints:

$$g_i(\tau_i) = 1 - \bar{T}(\tau_i)/T_a \qquad (i = 1, 2, \ldots, NT)$$

This approach has the disadvantage of increasing the number of constraints that need to be satisfied. The advantage of this approach is that careful control of the choice of the discrete time values can be exercised. Thus, after a design based on an initial choice of discrete times is obtained, a check can be made to see if violations occur between the discrete time values. If there are violations, the design may be repeated with a refined choice of $\tau_i$ in the region of the violations.

## Incorporation of Temperature Control Devices

Changing areas of bar elements and thicknesses of membrane elements is a relatively weak thermal control procedure. It is recognized that practical control of heated structures requires more effective thermal control devices such as forced-convection active cooling systems (ref. 12). The number of possible design variables necessary to characterize these systems is potentially large and includes, for example, the sizes, spacing and shape of coolant passages. The mass penalties include structural mass, coolant inventory mass as well as pumping penalties. Incorporation of this type of thermal control is desirable for effective thermal optimization, but appropriate characterizations of these systems are required before they can be incorporated into an overall optimization scheme for thermal/mechanical design.

## Thermal Stress Relief Mechanisms

In reference 3, a method was developed for identifying situations where fully-stressed design procedures for structures under prescribed temperatures and mechanical loads would fail unless thermal stresses are reduced by means other than resizing. In that reference, a factor $\beta$ was computed as the largest fraction of the thermal stress that could be accommodated in each element. No attempt was made either to relate $\beta$ to a physical thermal stress reduction mechanism or to assign a mass penalty to the value of $\beta$.

Thermal stress reduction can often be achieved by allowing expansion at potentially highly thermally-stressed portions of structures. For example, expansion joints have been proposed in the design of thermally-loaded piping systems (ref. 13), and candidate thermal protection systems for space transportation-type vehicles are typically attached to the substructure by flexible

supports (ref. 14). Panels of tubular construction have been proposed for high-temperature applications because the curved shapes allow thermal expansion without significant thermal stresses (ref. 15). Relating $\beta$ to an appropriate expansion device with an appropriate penalty could enhance the thermal/mechanical optimization procedure.

## CONCLUDING REMARKS

This report describes a finite-element based methodology for minimum-mass design of structures subjected to combined thermal-mechanical loading and both strength and thermal requirements. To simplify the development, temperatures were assumed to be steady-state and controlled by structural sizes only. A mathematical programming method based on the Sequence of Unconstrained Minimizations Technique (SUMT) was used in which design requirements are represented by an exterior penalty function. Temperatures were treated as behavior variables rather than fixed load-type quantities and temperatures were updated during resizing by finite element analyses.

Design calculations were performed for a wing box with both mechanical loading and external heating and subject to design constraints on stress, minimum gage, and temperature. Optimum designs without temperature constraints were also obtained. Temperature constraints had a significant effect on both the distribution of structural material and the total mass in the final design.

Some additional developments beyond the scope of the present work but needed for design of practical aerospace structures under realistic load situations are identified. Among these developments are design-oriented transient thermal analysis capability, treatment of time-dependent constraints, and incorporation of effective temperature control devices and thermal-stress relieving mechanisms.

# APPENDIX A

## THERMAL ANALYSIS FINITE ELEMENTS

The conductivity matrix and the thermal force vector for the bar and triangular finite elements are obtained by standard finite element methods (ref. 16). It is necessary to start with a functional expressed in terms of temperatures which, when minimized according to the usual calculus of variations methods, yields the matrix equations governing the temperature distribution. The functional appropriate to three-dimensional heat conductions, including convection and surface heat-load effects, is

$$U = \frac{1}{2}\int_V \left\{\nabla T\right\}^T \left[k\right] \left\{\nabla T\right\} dV + \int_S \left[H\left(\frac{T^2}{2} - T T_\infty\right) - q T\right] dS \qquad (A1)$$

where $[k]$ thermal conductivity matrix

$T$ temperature

$\{\nabla T\}$ temperature gradient vector $= \left[\frac{\partial T}{\partial x}, \frac{\partial T}{\partial y}, \frac{\partial T}{\partial z}\right]^T$

$V$ volume of finite element

$H$ convective heat transfer coefficient

$T_\infty$ ambient temperature at surface of finite element

$S$ surface of finite element

$q$ heat flux over surface of element

### Bar Element

The functional of equation (A1) for a one-dimensional element (bar) has the following form:

$$U = \int_0^{\ell} \left[ \frac{k}{2} A \left( \frac{\partial T}{\partial x} \right)^2 + HP \left( \frac{T^2}{2} - TT_{\infty} \right) - qT \right] dx$$

$$- q_1 A T_1 - q_2 A T_2 + H_1 A \left( \frac{T_1^2}{2} - T_1 T_{\infty 1} \right) + H_2 A \left( \frac{T_2^2}{2} - T_2 T_{\infty 2} \right) \qquad \text{(A2)}$$

The terms in equation (A2) are defined with reference to figure 6(a).

| | |
|---|---|
| $A$ | cross-sectional area of bar |
| $P$ | perimeter of bar cross-section |
| $T_{\infty}$, $T_{\infty 1}$, $T_{\infty 2}$ | ambient temperature adjacent to lateral surface of bar and end points 1 and 2, respectively |
| $T_1$ and $T_2$ | temperatures at bar end points 1 and 2, respectively |
| $H$, $H_1$, $H_2$ | convective heat transfer coefficient for medium adjacent to lateral surface of the bar and at end points 1 and 2, respectively |
| $q$, $q_1$, $q_2$ | heat flux at lateral surface of bar and end points 1 and 2, respectively |

The temperature distribution along the bar is assumed to be linear, thus

$$T = T_1 + \left( \frac{T_2 - T_1}{\ell} \right) x \qquad \text{(A3)}$$

Substituting equation (A3) into (A2) gives

$$U = \frac{1}{2} \{T\}^T [K]_b \{T\} - \{T\}^T \{L\}_b \qquad \text{(A4)}$$

where

$$\{T\} = \begin{Bmatrix} T_1 \\ T_2 \end{Bmatrix} \qquad \text{(A5)}$$

$$[K]_b = \begin{bmatrix} \frac{kA}{\ell} + \frac{HP\ell}{3} + H_1 A & -\frac{kA}{\ell} + \frac{HP\ell}{6} \\ -\frac{kA}{\ell} + \frac{HP\ell}{6} & \frac{kA}{\ell} + \frac{HP\ell}{3} + H_2 A \end{bmatrix} \tag{A6}$$

$$\{L\}_b = \begin{Bmatrix} \frac{HP\ell T_\infty}{2} + \frac{q\ell}{2} + q_1 A + H_1 A T_{\infty 1} \\ \frac{HP\ell T_\infty}{2} + \frac{q\ell}{2} + q_2 A + H_2 A T_{\infty 2} \end{Bmatrix} \tag{A7}$$

The matrix $[K]_b$ and the vector $\{L\}_b$ denote the conductivity matrix and the thermal force vector, respectively, for the bar element.

## Triangular Element

The functional in equation (A1) for two-dimensional heat transfer over a triangular region has the following form:

$$\begin{aligned} U = & \int_\Delta \frac{1}{2} \left[ k_x \left( T_{,x} \right)^2 + k_y \left( T_{,y} \right)^2 + 2 k_{xy} T_{,x} T_{,y} \right] h \, dx \, dy \\ & + \int_\Delta \left[ H \left( \frac{T^2}{2} - T T_\infty \right) - qT \right] dx \, dy \\ & + \int_{S_1} \left[ H_1 \left( \frac{T^2}{2} - T T_{\infty 1} \right) - q_1 T \right] h \, ds_1 + \int_{S_2} \left[ H_2 \left( \frac{T^2}{2} - T T_{\infty 2} \right) - q_2 T \right] h \, ds_2 \\ & + \int_{S_3} \left[ H_3 \left( \frac{T^2}{2} - T T_{\infty 3} \right) - q_3 T \right] h \, ds_3 \end{aligned} \tag{A8}$$

where

| | |
|---|---|
| $k_x$, $k_y$, $k_{xy}$ | thermal conductivities with respect to coordinate directions in the plane of the element (fig. 6(b)) |
| $T_{,x}$ | $\frac{\partial T}{\partial x}$, component of temperature gradient in x-direction |
| $T_{,y}$ | $\frac{\partial T}{\partial y}$, component of temperature gradient in y-direction |
| $H$, $H_1$, $H_2$, $H_3$ | convective heat transfer coefficients corresponding to the media adjacent to the surface of the element and the three edges of the element, respectively |
| $T_\infty$, $T_{\infty 1}$, $T_{\infty 2}$, $T_{\infty 3}$ | ambient temperatures corresponding to the surface of the element and edges 1, 2, and 3, respectively |
| $q$, $q_1$, $q_2$, $q_3$ | heat flux normal to surface of the element and normal to edges 1, 2, and 3, respectively |
| $\Delta$ | area of the triangular element |
| $s_1$, $s_2$, $s_3$ | edges of the triangular element |

Equation (A8) may be written more compactly as:

$$
\begin{aligned}
U = \frac{1}{2} \int_{\Delta} \begin{Bmatrix} T \\ T_{,x} \\ T_{,y} \end{Bmatrix}^T \begin{bmatrix} k \end{bmatrix} \begin{Bmatrix} T \\ T_{,x} \\ T_{,y} \end{Bmatrix} dx\, dy \\
- \int \begin{Bmatrix} T \\ T_{,x} \\ T_{,y} \end{Bmatrix}^T \begin{Bmatrix} \Omega \end{Bmatrix} dx\, dy \\
+ \int_{s_1} \left[ H_1 \left( \frac{T^2}{2} - T T_{\infty 1} \right) - q_1 T \right] h\, ds_1 \\
+ \int_{s_2} \left[ H_2 \left( \frac{T^2}{2} - T T_{\infty 2} \right) - q_2 T \right] h\, ds_2 \\
+ \int_{s_3} \left[ H_3 \left( \frac{T^2}{2} - T T_{\infty 3} \right) - q_3 T \right] h\, ds_3
\end{aligned}
\tag{A9}
$$

where

$$[k] = \begin{bmatrix} H & 0 & 0 \\ 0 & k_x h & k_{xy} h \\ 0 & k_{xy} h & k_y h \end{bmatrix} \tag{A10}$$

$$\{\Omega\} = \begin{Bmatrix} q + HT_\infty \\ 0 \\ 0 \end{Bmatrix} \tag{A11}$$

The temperature distribution is assumed to vary quadratically over the element as follows

$$T = a_0 + a_1 x + a_2 y + a_3 xy + a_4 x^2 + a_5 y^2 \tag{A12}$$

The coefficients in (A12) may be expressed in terms of the temperatures and x, y coordinates at the six grid points of the element. This relationship is written in matrix form as

$$\{a\} = [Q]\{T\} \tag{A13}$$

where

$$\{a\}^T = \begin{bmatrix} a_0 & a_1 & a_2 & a_3 & a_4 & a_5 \end{bmatrix} \tag{A14}$$

$$\{T\}^T = \begin{bmatrix} T_1 & T_2 & T_3 & T_4 & T_5 & T_6 \end{bmatrix} \tag{A15}$$

$$[Q] = \begin{bmatrix} 1 & x_1 & y_1 & x_1 y_1 & x_1^2 & y_1^2 \\ 1 & x_2 & y_2 & x_2 y_2 & x_2^2 & y_2^2 \\ 1 & x_3 & y_3 & x_3 y_3 & x_3^2 & y_3^2 \\ 1 & x_4 & y_4 & x_4 y_4 & x_4^2 & y_4^2 \\ 1 & x_5 & y_5 & x_5 y_5 & x_5^2 & y_5^2 \\ 1 & x_6 & y_6 & x_6 y_6 & x_6^2 & y_6^2 \end{bmatrix}^{-1} \tag{A16}$$

Substitution of equation (A12) into (A9) and use of equations (A13) through (A15) yields:

$$U = \frac{1}{2}\{T\}^T[K]_m\{T\} - \{T\}^T\{L\}_m \tag{A17}$$

where

$$[K]_m = [Q]^T\int_\Delta [X]^T[k]\,[X]\,dx\,dy\;\;[Q] + [Q]^T\left(\frac{H_1h}{2}\int_{s_1}\{Y\}^T\{Y\}\,ds_1 + \frac{H_2h}{2}\int_{s_2}\{Y\}^T\{Y\}\,ds_2 + \frac{H_3h}{2}\int_{s_3}\{Y\}^T\{Y\}\,ds_3\right)[Q] \tag{A18}$$

$$\{L\}_m = [Q]^T\int_\Delta [X]^T\left\{\mathcal{Q}\right\}dx\,dy + h\,[Q]^T\left((q_1 + H_1T_{\infty1})\int_{s_1}\{Y\}^T\,ds_1 + (q_2 + H_2T_{\infty2})\int_{s_2}\{Y\}^T\,ds_2 + (q_3 + H_3T_{\infty3})\int_{s_3}\{Y\}^T\,ds_3\right) \tag{A19}$$

$$[X] = \begin{bmatrix} 1 & x & y & xy & x^2 & y^2 \\ 0 & 1 & 0 & y & 2x & 0 \\ 0 & 0 & 1 & x & 0 & 2y \end{bmatrix} \tag{A20}$$

$$\{Y\}^T = \begin{bmatrix} 1 & x & y & xy & x^2 & y^2 \end{bmatrix} \tag{A21}$$

The integration indicated by $\int_\Delta$ is performed in closed form using triangular integration according to formulas given in reference 17. The line integrals indicated by $\int_{s_1}$, $\int_{s_2}$, and $\int_{s_3}$ are performed in closed form making use of the equations of the straight lines defining sides 1, 2, and 3.

The conductivity matrix and thermal force vector for the triangular element are identified as $[K]_m$ and $\{L\}_m$, respectively. Having derived the conductivity matrix and thermal force vector for the bars and membranes, it is a simple matter to assemble the corresponding matrix and vector for the complete structure by the standard finite element method. The resulting matrix and vector are denoted $[\overline{K}]$ and $\{\overline{L}\}$ as used in equation (5) of the main text.

## APPENDIX B

## GRADIENT OF PENALTY FUNCTION

Expressions for the components of the gradient of the penalty function (eq. 6) are summarized in this appendix. The required gradient is

$$\nabla \phi = \nabla \left( m + r \sum_{j=1}^{nc} < g_j >^2 \right) \tag{B1}$$

where $m$ is the total mass of the structure and the $g_j$ are constraints defined in equations (8)-(13) of the main text. For convenience in notation, the vector of design variables $\{t\}$ is defined as follows:

$$\{t\}_{nx1} = \begin{Bmatrix} \{A\}_{nb \times 1} \\ \{h\}_{nm \times 1} \end{Bmatrix} \tag{B2}$$

where $\{A\}$ is the vector of $nb$ bar cross-sectional areas
$\{h\}$ is the vector of $nm$ membrane thicknesses.

Thus,

$$m = m(\{t\}) = \sum_{i=1}^{n} \rho_i \ell_i t_i \tag{B3}$$

where $\rho_i$ is the density of the i-th design variable and $\ell_i$ is the length of a bar element or planform area of a membrane element. Combining equations (B1) and (B3) leads to the following expression for the i-th component of the gradient:

$$\frac{\partial \phi}{\partial t_i} = \rho_i \ell_i + 2r \sum_{j=1}^{nc} \left[\frac{\partial g_j}{\partial t_i}\right] \{\langle g_j \rangle\} \qquad \text{(B4)}$$

The remaining task is to obtain expressions for $\frac{\partial g_j}{\partial t_i}$. These expressions are summarized for each of the six types of constraints (eqs. (8)-(13)).

## Bar Stress Constraints

Using equations (1), (2), and (8)

$$\frac{\partial g_j}{\partial t_i} = \frac{-1}{\sigma_a} \lfloor B_j \rfloor \left\{\frac{\partial u}{\partial t_i}\right\}_j + \left(\frac{E\alpha}{\sigma_a}\right)_j \frac{\partial \bar{T}_j}{\partial t_i}$$

$$(j = 1, 2, \ldots, nb) \qquad \text{(B5)}$$

where $\left\{\frac{\partial u}{\partial t_i}\right\}_j$ is the appropriate 6 x 1 sub-vector of

$$\left\{\frac{\partial U}{\partial t}\right\} = [K]^{-1} \left( \left\{\frac{\partial L}{\partial t}\right\} - \left[\frac{\partial K}{\partial t}\right] \{U\} \right) \qquad \text{(B6)}$$

associated with the two ends of the bar

and $\frac{\partial \bar{T}}{\partial t}$ is the appropriate 2 x 1 sub-vector of

$$\left\{\frac{\partial T}{\partial t}\right\} = [K]^{-1} \left( \left\{\frac{\partial \bar{L}}{\partial t}\right\} - \left[\frac{\partial R}{\partial t}\right] \{T\} \right) \qquad \text{(B7)}$$

associated with the temperatures at the two ends of the bar.

## Bar Minimum-Gage Constraints

Using equation (9):

$$\frac{\partial g_j}{\partial t_i} = \frac{A_{min}}{t_i^2} \delta_{i,j-nb} \qquad (j = nb+1, nb+2, \ldots, 2nb) \qquad (B8)$$

where $\delta_{i,j-nb}$ is the Kronecker delta.

## Bar Temperature Constraints

Using equation (10):

$$\frac{\partial g_j}{\partial t_i} = - \frac{1}{T_a} \frac{\partial \bar{T}_{j-2nb}}{\partial t_i} \qquad (j = 2nb+1, 2nb+2, \ldots, 3nb) \qquad (B9)$$

## Membrane Stress Constraints

Using equations (3), (4), and (11):

$$\frac{\partial g_j}{\partial t_i} = - \frac{1}{\sigma_a} \frac{\partial V_{j-3nb}}{\partial t_i} \qquad (j = 3nb+1, 3nb+2, \ldots, 3nb+nm)$$

where, for every membrane element

$$\frac{\partial V}{\partial t} = \lfloor C \rfloor \left\{ \frac{\partial u}{\partial t} \right\} - S \qquad (B10)$$

$$\lfloor C \rfloor = \left( \frac{2\sigma_x - \sigma_y}{2V} \right) \lfloor C_x \rfloor + \left( \frac{2\sigma_y - \sigma_x}{2V} \right) \lfloor C_y \rfloor + \frac{3\sigma_{xy}}{V} \lfloor C_{xy} \rfloor \qquad (B11)$$

$$S = \left[ \left( \frac{2\sigma_x - \sigma_y}{2V} \right) G_x + \left( \frac{2\sigma_y - \sigma_x}{2V} \right) G_y + \frac{3\sigma_{xy}}{V} G_{xy} \right] \frac{\partial \bar{T}}{\partial t} \qquad \text{(B12)}$$

Membrane Minimum Gage Constraints

From equation (12):

$$\frac{\partial g_j}{\partial t_i} = \frac{h_{min}}{t_i^2} \delta_{i,j-3nb-nm} \quad (j = 3nb+nm+1, 3nb+nm+2, \ldots, 3nb+2nm) \qquad \text{(B13)}$$

Membrane Temperature Constraints

From equation (13):

$$\frac{\partial g_j}{\partial t_i} = -\frac{1}{T_i} \frac{\partial \bar{T}_{j-3nb-2nm}}{\partial t_i}$$

$$(j = 3nb+2nm+1, 3nb+2nm+2, \ldots, 3(nb+nm)) \qquad \text{(B14)}$$

## REFERENCES


1. Schmit, L. A.; and Muira, H.: An Advanced Structural Analysis/Synthesis Capability - ACCESS 2. Proceedings of the 17th Structures, Structural Dynamics and Materials Conf., AIAA, King of Prussia, PA, May 5-7, 1976, pp. 432-447.

2. Gellatly, R. A.; Gallagher, R. H.; and Luberacki, W. A.: Development of a Procedure for Automated Synthesis of Minimum Weight Structures. FDL-TDR-64-141, U.S. Air Force, Oct. 1964. (Available from DDC as AD 611 310).

3. Adelman, Howard M.; Walsh, Joanne L.; and Narayanaswami, R.: An Improved Method for Optimum Design of Mechanically and Thermally Loaded Structures. NASA TN D-7965, 1975.

4. Thornton, W. A.; and Schmit, L. A.: The Structural Synthesis of an Ablating Thermostructural Panel. NASA CR-1215, Dec. 1968.

5. Hackman, L. E.; and Richardson, J. E.: Design Optimization of Aircraft Structures with Thermal Gradients. Paper No. 63-9, presented at 31st Annual Meeting, New York, Jan. 21-23, 1963.

6. Fox, Richard L.: Optimization Methods for Engineering Design. Addison-Wesley Pub. Co., Inc., c. 1971.

7. Argyris, J. H.: Triangular Elements with Linearly Varying Strain for the Matrix Displacement Method. Journal of the Royal Aeronautical Society, Vol. 69, Oct. 1965.

8. Davidon, W. C.: Variance Algorithm for Minimization. Computer Journal, Vol. 10, No. 4, Feb. 1968, pp. 406-411.

9. Fletcher, R.; and Powell, M.J.D.: A Rapidly Convergent Descent Method for Minimization. The Computer Journal, Vol. 6, 1959, p. 163.

10. Lee, H. P.: The NASTRAN Thermal Analyzer Manual. NASA, Goddard Space Flight Center X-322-76-16, Dec. 1974.

11. Storaasli, O. O.; and Sobieszczanski, J.: On the Accuracy of the Taylor Approximation for Structural Resizing. AIAA J., Vol. 12, No. 2, Feb. 1974, pp. 231-233.

12. Nowak, Robert J.; and Kelly, H. Neale: Actively Cooled Airframe Structures For High-Speed Flight. J. Aircraft, Vol. 14, No. 3, March 1977, pp. 244-250.

13. Fenton, R. G.: Stress Analysis of Pipelines Fitted With Expansion Devices. 74-WA/PVP-10, American Soc. Mech. Eng., Nov. 1974.

14. Bohon, Herman L.; Sawyer, J. Wayne; Hunt, L. Roane; and Weinstein, Irving: Performance of a Thermal Protection System in a Mach 7 Environment. J. Spacecraft and Rockets, Vol. 12, No. 12, Dec. 1975, pp. 744-749.

15. Shideler, John L.; and Bohon, Herman L.: Evaluation of Bead-Stiffened Metal Panels, J. of Spacecraft and Rockets, Vol. 13, No. 3, March 1976, pp. 144-149.

16. Zienciewicz, O. C.: The Finite Element Method in Structural and Continuum Mechanics. McGraw-Hill Co., Ltd., c. 1967.

17. Bell, K.: Triangular Plate Bending Elements. Finite Element Methods in Stress Analysis. Holland, Ivar; and Bell, Kolbein; editors, Tapier (Trondheim, Norway), 1969, pp. 213-252.

TABLE 1. - SUMMARY OF APPLIED LOADS, BOUNDARY CONDITIONS AND MATERIAL PROPERTIES FOR WING BOX

(a) LOADS

| | | UPPER SURFACE | LOWER SURFACE |
|---|---|---|---|
| $N_x$ | N/m | -38* | -452 |
| | lbf/in | -336 | -4000 |
| | | | |
| $N_y$ | N/m | -136 | 147 |
| | lbf/in | -1200 | 1300 |
| | | | |
| $N_{xy}$ | N/m | 60 | 14 |
| | lbf/in | 528 | 128 |
| | | | |
| p | Pa | 276 | 6895 |
| | psi | .04 | 1.0 |
| | | | |
| Q | $Watt/m^2$ | 0 | 1.634 |
| | $BTU/in^2sec$ | 0 | $1 \times 10^{-6}$ |

*(minus sign → compression)

(b) BOUNDARY CONDITIONS

| | |
|---|---|
| Edge 1 | T = 987 K (1300°F) |
| Edge 2 | T = 1061 K (1450°F) |
| Edge 3 | T = 916 K (1270°F), u = v = w = 0 |
| Edge 4 | T = 1047 K (1425°F), u = v = w = 0 |

(c) MATERIAL PROPERTIES

| | |
|---|---|
| E = 193 GPa ($28 \times 10^6$psi) | $\sigma_a$ = 875 MPa (127 ksi) |
| $\rho$ = 8248 $kg/m^3$(0.298 $lbm/in^3$) | $\alpha = 13.8 \times 10^{-6}/K$ ($7.5 \times 10^{-6}$/°F) |
| $\nu$ = .30 | k = 15 W/m-s-K $\left(.0002 \frac{BTU}{in\text{-}s\text{-}°F}\right)$ |

TABLE 2. - GRID POINT COORDINATES OF WING BOX FINITE ELEMENT MODEL

| Grid Point | X | | Y | | Z | |
|---|---|---|---|---|---|---|
| | cm | in | cm | in | cm | in |
| 1 | 0 | 0 | 0 | 0 | 113.0 | 44.5 |
| 2 | 102 | 40 | 0 | 0 | 113.0 | 44.5 |
| 3 | 203 | 80 | 0 | 0 | 113.0 | 44.5 |
| 4 | 203 | 80 | 0 | 0 | 0 | 0 |
| 5 | 102 | 40 | 0 | 0 | 0 | 0 |
| 6 | 0 | 0 | 0 | 0 | 0 | 0 |
| 7 | 0 | 0 | 102 | 40 | 113.0 | 44.5 |
| 8 | 102 | 40 | 102 | 40 | 113.0 | 44.5 |
| 9 | 203 | 80 | 102 | 40 | 113.0 | 44.5 |
| 10 | 203 | 80 | 102 | 40 | 0 | 0 |
| 11 | 102 | 40 | 102 | 40 | 0 | 0 |
| 12 | 0 | 0 | 102 | 40 | 0 | 0 |
| 13 | 0 | 0 | 203 | 80 | 113.0 | 44.5 |
| 14 | 102 | 40 | 203 | 80 | 113.0 | 44.5 |
| 15 | 203 | 80 | 203 | 80 | 113.0 | 44.5 |
| 16 | 203 | 80 | 203 | 80 | 0 | 0 |
| 17 | 102 | 40 | 203 | 80 | 0 | 0 |
| 18 | 0 | 0 | 203 | 80 | 0 | 0 |
| 19 | 0 | 0 | 305 | 120 | 113.0 | 44.5 |
| 20 | 102 | 40 | 305 | 120 | 113.0 | 44.5 |
| 21 | 203 | 80 | 305 | 120 | 113.0 | 44.5 |
| 22 | 203 | 80 | 305 | 120 | 0 | 0 |
| 23 | 102 | 40 | 305 | 120 | 0 | 0 |
| 24 | 0 | 0 | 305 | 120 | 0 | 0 |
| 25 | 0 | 0 | 406 | 160 | 113.0 | 44.5 |
| 26 | 102 | 40 | 406 | 160 | 113.0 | 44.5 |
| 27 | 203 | 80 | 406 | 160 | 113.0 | 44.5 |
| 28 | 203 | 80 | 406 | 160 | 0 | 0 |
| 29 | 102 | 40 | 406 | 160 | 0 | 0 |
| 30 | 0 | 0 | 406 | 160 | 0 | 0 |

TABLE 3. - APPLIED MECHANICAL FORCES AT GRID POINTS OF WING BOX FINITE ELEMENT MODEL

| Grid Point | $P_x$ | | $P_y$ | | $P_z$ | |
|---|---|---|---|---|---|---|
| | N | lbf | N | lbf | N | lbf |
| 1 | - 11387 | - 2560 | 39856 | 8960 | - 49 | -11 |
| 2 | -125262 | - 28160 | 248686 | 64000 | - 71 | -16 |
| 3 | - 51244 | - 11520 | 102487 | 23040 | - 22 | - 5 |
| 4 | -244830 | - 55040 | - 69499 | -15624 | 592 | 133 |
| 5 | - 30372 | - 6828 | -308404 | -69332 | 1779 | 400 |
| 6 | 229635 | 51624 | - 84694 | -19040 | 1188 | 267 |
| 7 | 79712 | 17920 | -125262 | -28160 | - 71 | -16 |
| 8 | 0 | 0 | 0 | 0 | -142 | -32 |
| 9 | - 79712 | - 17920 | 125262 | 28160 | - 71 | -16 |
| 10 | -948948 | -213332 | 30372 | 6828 | 1779 | 400 |
| 11 | 0 | 0 | 0 | 0 | 3559 | 800 |
| 12 | 948948 | 213332 | - 30372 | - 6828 | 1779 | 400 |
| 13 | 39856 | 8960 | - 62631 | -14080 | - 71 | -16 |
| 14 | 0 | 0 | 0 | 0 | -142 | -32 |
| 15 | - 39856 | - 8960 | 62631 | 14080 | - 71 | -16 |
| 16 | -474483 | -106668 | 15177 | 3412 | 1779 | 400 |
| 17 | 0 | 0 | 0 | 0 | 3559 | 800 |
| 18 | 474483 | 106668 | - 15177 | - 3412 | 1779 | 400 |
| 19 | 79712 | 17920 | -125262 | -28160 | - 71 | -16 |
| 20 | 0 | 0 | 0 | 0 | -142 | -32 |
| 21 | - 79712 | - 17920 | 125262 | 28160 | - 71 | -16 |
| 22 | -948948 | -213332 | 30372 | 6828 | 1779 | 400 |
| 23 | 0 | 0 | 0 | 0 | 3559 | 800 |
| 24 | 948948 | 213332 | - 30372 | - 6828 | 1779 | 400 |

TABLE 4. - MECHANICAL AND THERMAL BOUNDARY CONDITIONS FOR WING BOX MODEL

| Grid Point | Displacement Boundary Condition | Thermal Boundary Condition |
|---|---|---|
| 1 | free | T = 978 K (1300°F) |
| 2 | ↓ | ↓ |
| 3 | ↓ | ↓ |
| 4 | ↓ | T = 1061 K (1450°F) |
| 5 | ↓ | ↓ |
| 6 | ↓ | ↓ |
| 25 | u = v = w = 0 | T = 961 K (1270°F) |
| 26 | ↓ | ↓ |
| 27 | ↓ | ↓ |
| 28 | ↓ | T = 1047 K (1425°F) |
| 29 | ↓ | ↓ |
| 30 | ↓ | ↓ |

TABLE 5. - FINAL DESIGN OF WING BOX INCLUDING STRENGTH AND TEMPERATURE CONSTRAINTS

(a) BAR AREAS

| Bar | Area | | Bar | Area | | Bar | Area | |
|---|---|---|---|---|---|---|---|---|
| | $cm^2$ | $in^2$ | | $cm^2$ | $in^2$ | | $cm^2$ | $in^2$ |
| 1 | .6232 | .0966 | 24 | .1639 | .0254 | 47 | .1135 | .0176 |
| 2 | .1284 | .0199 | 25 | .6200 | .0961 | 48 | .1439 | .0223 |
| 3 | .5871 | .0910 | 26 | .0684 | .0106 | 49 | .0645 | .0100 |
| 4 | .1548 | .0240 | 27 | .3684 | .0571 | 50 | .0877 | .0136 |
| 5 | .1381 | .0214 | 28 | 1.7123 | .2654 | 51 | .4994 | .0774 |
| 6 | .0916 | .0142 | 29 | .3568 | .0553 | 52 | .0710 | .0110 |
| 7 | .1574 | .0244 | 30 | 1.7445 | .2704 | 53 | .4471 | .0693 |
| 8 | .0690 | .0107 | 31 | 2.2090 | .3424 | 54 | .2239 | .0347 |
| 9 | 2.2529 | .3492 | 32 | .1194 | .0185 | 55 | .0652 | .0101 |
| 10 | .3619 | .0561 | 33 | .1303 | .0202 | 56 | .1084 | .0168 |
| 11 | .1374 | .0213 | 34 | .0806 | .0125 | 57 | .8426 | .1306 |
| 12 | 2.6697 | .4138 | 35 | .5174 | .0802 | 58 | .0942 | .0146 |
| 13 | .0794 | .0123 | 36 | .3948 | .0612 | 59 | .0665 | .0103 |
| 14 | .0742 | .0115 | 37 | .1832 | .0284 | 60 | .0742 | .0115 |
| 15 | .0652 | .0101 | 38 | .1529 | .0237 | 61 | .0877 | .0136 |
| 16 | .0755 | .0117 | 39 | .1013 | .0157 | 62 | 1.8413 | .2854 |
| 17 | .1161 | .0180 | 40 | .0826 | .0128 | 63 | .1032 | .0160 |
| 18 | .0774 | .0120 | 41 | .0652 | .0101 | 64 | .1174 | .0182 |
| 19 | .8600 | .1333 | 42 | .1123 | .0174 | 65 | .4555 | .0706 |
| 20 | .2748 | .0426 | 43 | .0852 | .0132 | 66 | .3490 | .0541 |
| 21 | .1974 | .0306 | 44 | .1768 | .0274 | 67 | 2.4032 | .3725 |
| 22 | .0819 | .0127 | 45 | .0774 | .0120 | 68 | 2.6858 | .4163 |
| 23 | .4568 | .0708 | 46 | .3703 | .0574 | | | |

(b) MEMBRANE THICKNESSES

| Membrane | Thickness | | Membrane | Thickness | |
|---|---|---|---|---|---|
| | cm | in | | cm | in |
| 1 | .0630 | .0248 | 5 | 1.3861 | .5457 |
| 2 | .0513 | .0202 | 6 | .2769 | .1090 |
| 3 | .0257 | .0101 | 7 | .7488 | .2948 |
| 4 | .0269 | .0106 | 8 | .0935 | .0368 |

Final Mass = 485 kg (1070 lbm)

TABLE 6. - STATUS OF CONSTRAINTS IN WING BOX DESIGN

| (a) WING BOX WITH TEMPERATURE CONSTRAINTS | | | |
|---|---|---|---|
| Stress Critical | | Temperature Critical | |
| Bars | Membranes | Bars | Membranes |
| 19 | 1, 4, 5 | 19, 20, 23, 24, 27, 33, 34, 35, 42, 43, 49, 50, 51 | 6, 7, 8 |

| (b) WING BOX WITHOUT TEMPERATURE CONSTRAINTS | | | |
|---|---|---|---|
| Stress Critical | | Temperature Critical | |
| Bars | Membranes | Bars | Membranes |
| 19, 27, 63, 64 | 2, 5, 6, 8 | N.A. | N.A. |

## TABLE 7. - FINAL DESIGN OF WING BOX WITHOUT TEMPERATURE CONSTRAINTS

(a) BAR AREAS

| Bar | Area | | Bar | Area | | Bar | Area | |
|---|---|---|---|---|---|---|---|---|
| | $cm^2$ | $in^2$ | | $cm^2$ | $in^2$ | | $cm^2$ | $in^2$ |
| 1 | .0652 | .0101 | 24 | .2935 | .0455 | 47 | .0729 | .0113 |
| 2 | .0703 | .0109 | 25 | .1981 | .0307 | 48 | .0658 | .0102 |
| 3 | .0703 | .0109 | 26 | .2013 | .0312 | 49 | .0735 | .0114 |
| 4 | .0710 | .0110 | 27 | 1.548 | .2398 | 50 | .0652 | .0101 |
| 5 | .0845 | .0131 | 28 | .0729 | .0113 | 51 | .0664 | .0103 |
| 6 | .0710 | .0110 | 29 | .0910 | .0141 | 52 | .0645 | .0100 |
| 7 | .1245 | .0193 | 30 | .3032 | .0470 | 53 | .3439 | .0533 |
| 8 | .0697 | .0108 | 31 | .0652 | .0101 | 54 | .0677 | .0105 |
| 9 | .0645 | .0100 | 32 | .0748 | .0116 | 55 | .2310 | .0358 |
| 10 | .1742 | .0270 | 33 | .0761 | .0118 | 56 | .4942 | .0766 |
| 11 | .0645 | .0100 | 34 | .2052 | .0318 | 57 | .0845 | .0131 |
| 12 | .0774 | .0120 | 35 | .2806 | .0435 | 58 | .0684 | .0106 |
| 13 | .1252 | .0194 | 36 | .2052 | .0318 | 59 | .1013 | .0157 |
| 14 | .2361 | .0366 | 37 | .0645 | .0100 | 60 | .0658 | .0102 |
| 15 | .0677 | .0105 | 38 | .2858 | .0443 | 61 | .0710 | .0110 |
| 16 | .0748 | .0116 | 39 | .2632 | .0408 | 62 | .1955 | .0303 |
| 17 | .2574 | .0399 | 40 | .0852 | .0132 | 63 | .1864 | .0289 |
| 18 | .0910 | .0141 | 41 | .0671 | .0104 | 64 | .2426 | .0376 |
| 19 | 2.883 | .4472 | 42 | .0710 | .0110 | 65 | .4968 | .0770 |
| 20 | 3.974 | .6165 | 43 | .0910 | .0141 | 66 | .0658 | .0102 |
| 21 | .2858 | .0443 | 44 | .1974 | .0306 | 67 | .1413 | .0219 |
| 22 | .3884 | .0602 | 45 | .0664 | .0103 | 68 | .1600 | .0248 |
| 23 | .0671 | .0104 | 46 | .0645 | .0100 | | | |

(b) MEMBRANE THICKNESSES

| Membrane | Thickness | | Membrane | Thickness | |
|---|---|---|---|---|---|
| | cm | in | | cm | in |
| 1 | .0759 | .0299 | 5 | 1.0900 | .4290 |
| 2 | .0282 | .0111 | 6 | .1003 | .0395 |
| 3 | .0406 | .0160 | 7 | .0983 | .0387 |
| 4 | .0312 | .0123 | 8 | .0841 | .0331 |

Final Mass = 280 kg (617 lbm)

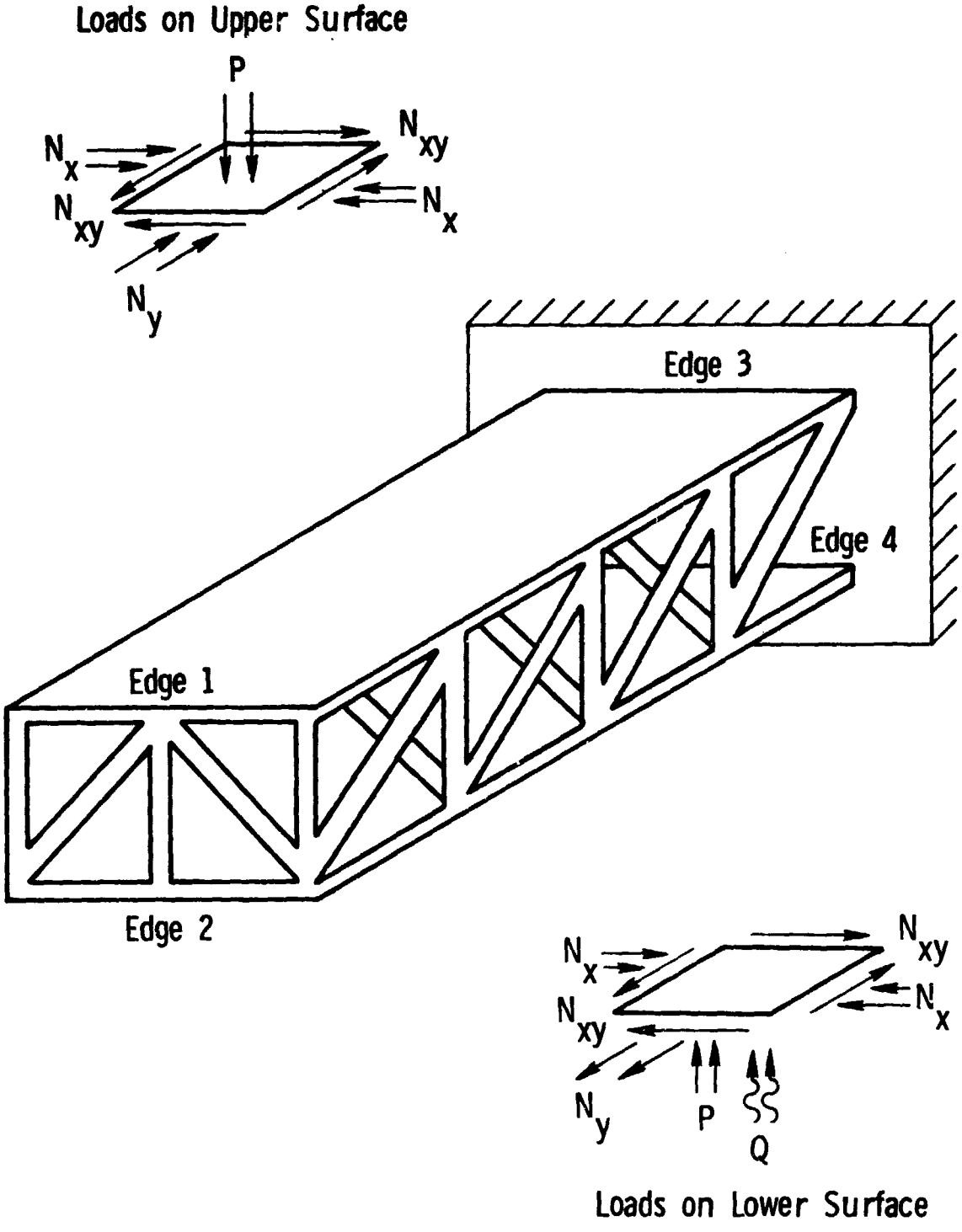


Figure 1.- Wing box model showing applied loads and edges where boundary conditions are specified (see table 1).

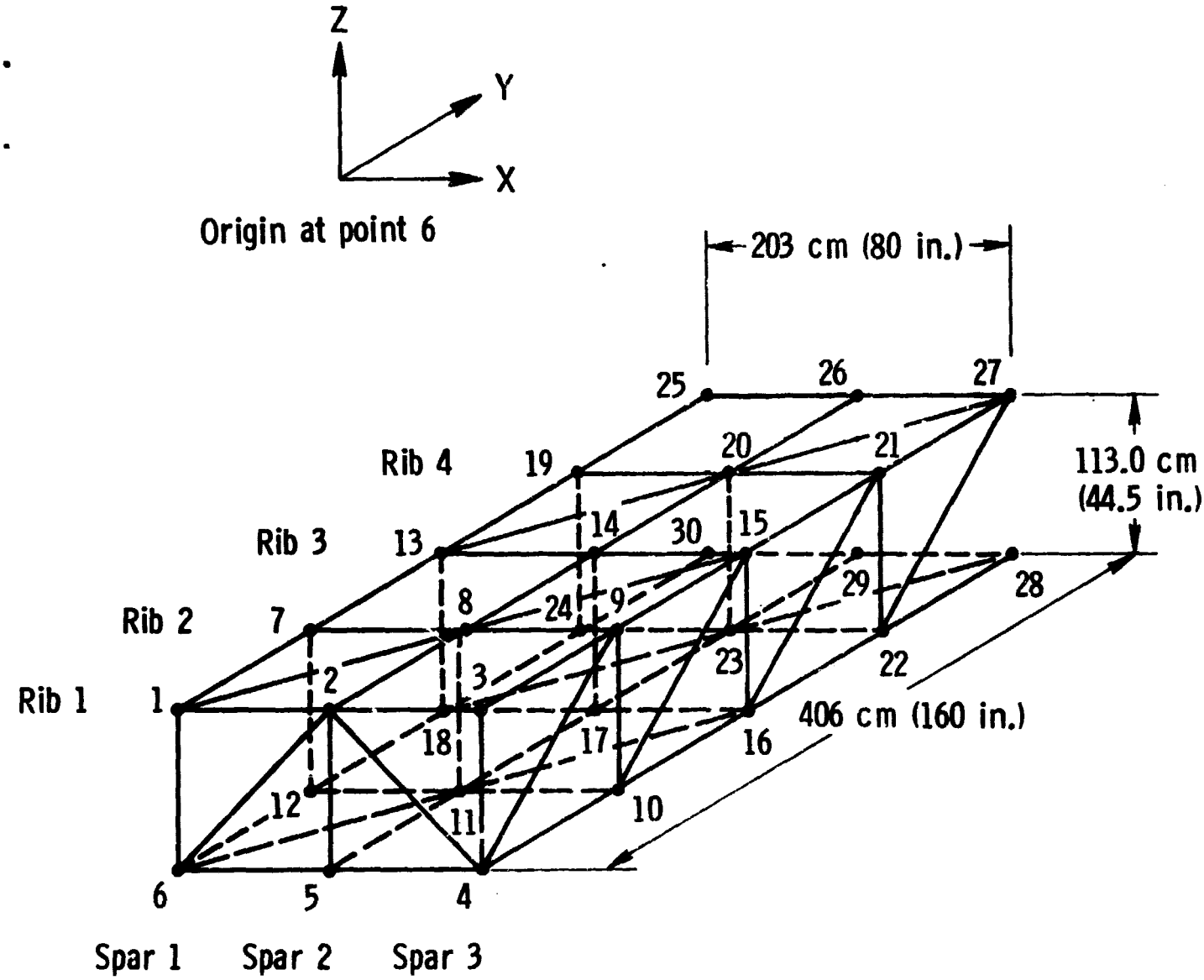


Figure 2.- Finite element model of wing box (for clarity not all elements are shown).

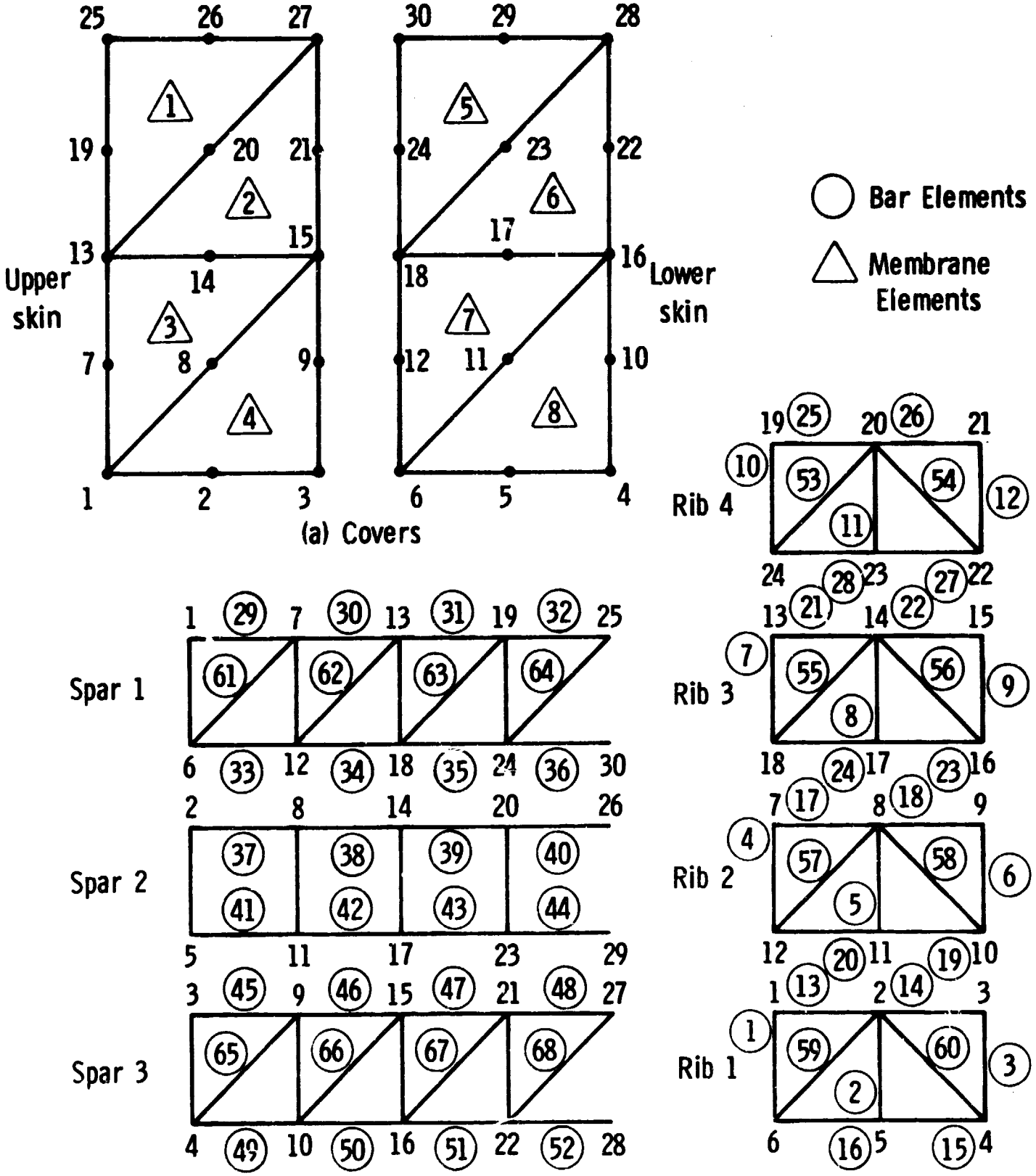


(a) Covers

(b) Ribs and Spars

Figure 3.- Detailed model of ribs, spars, and covers.

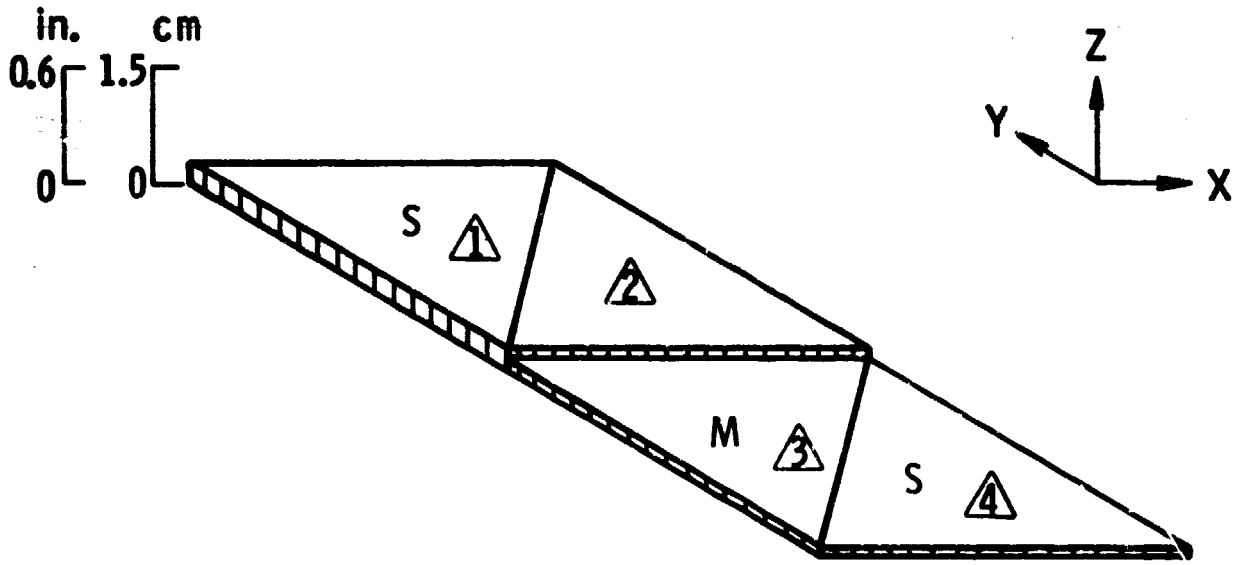


(a) Upper skin

S indicates stress-critical
T indicates temperature-critical
M indicates minimum gage

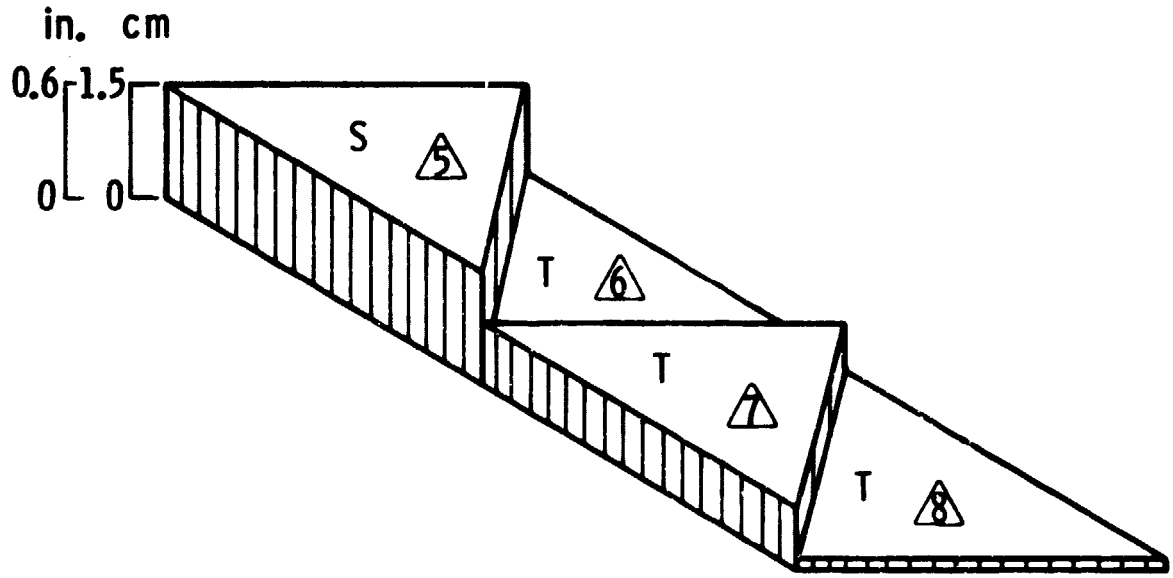


(b) Lower skin

Figure 4.- Distribution of membrane thickness in final design of wing box with temperature constraints included.

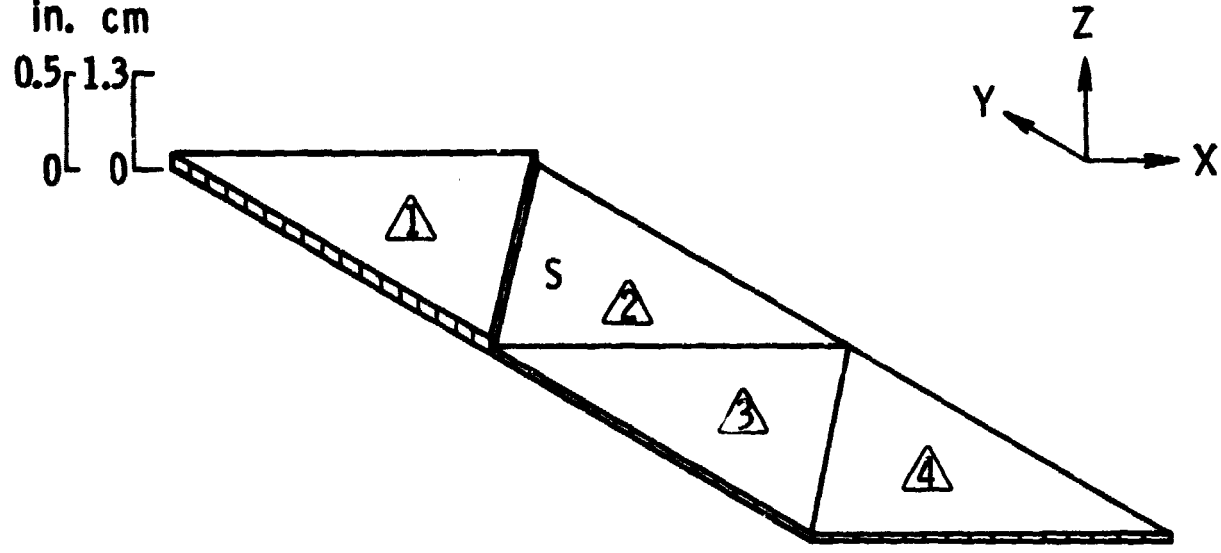


(a) Upper skin

S indicates stress-critical
M indicates minimum gage

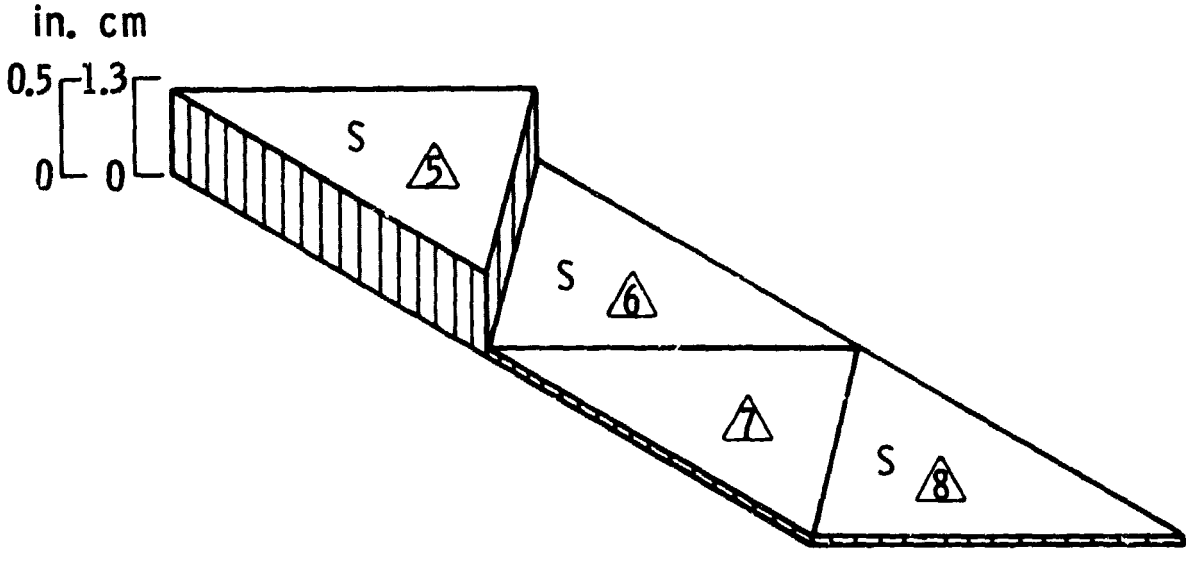


(b) Lower skin

Figure 5.- Distribution of membrane thickness in final design of wing box without temperature constraints.

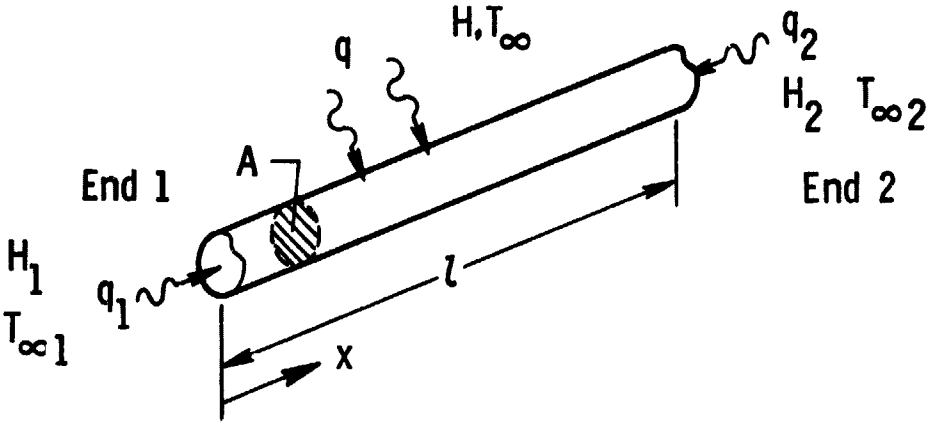


(a) Bar Element

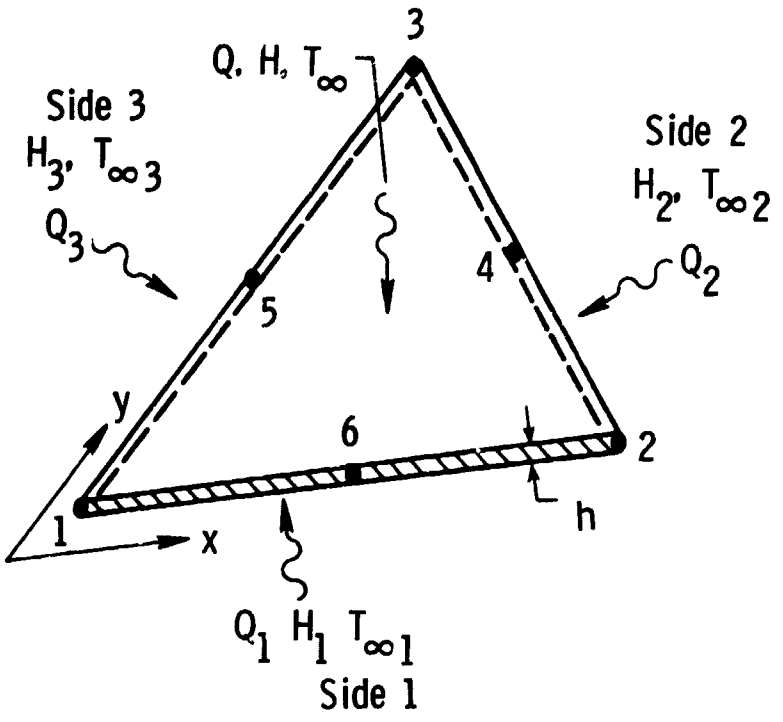


(b) Triangular Element

Figure 6.- Thermal finite elements.